# Dominant Formation of a Single-Length Channel by Amphotericin B in Dimyristoylphosphatidylcholine Membrane Evidenced by $^{13}C-^{31}P$ Rotational Echo Double Resonance†

Shigeru Matsuoka,‡,§ Hiroki Ikeuchi,‡ Nobuaki Matsumori,‡ and Michio Murata*,‡

*Department of Chemistry, Graduate School of Science, Osaka University, 1-16 Machikaneyama, Toyonaka, Osaka 560-0043, Japan, and CREST, Japan Science and Technology Corporaton, Osaka University, 1-16 Machikaneyama, Toyonaka, Osaka 560-0043, Japan*

*Received May 18, 2004; Revised Manuscript Received November 1, 2004*

ABSTRACT: $^{13}C$-Labeled amphotericin B (AmB) was prepared by feeding the producing organism *Streptomyces nodosus* with [3-$^{13}C$]propionate. The REDOR experiments for dimyristoylphosphatidylcholine (DMPC) membrane using the $^{13}C$-labeled AmB showed the prominent dephasing effects between the phosphate group in PC and C41 carboxyl carbon in the polar head. In addition, C39/C40 methyl carbons also gave rise to the significant reduction of their $^{13}C$ NMR signals, implying that both terminal parts of AmB reside close to the surface of the DMPC membrane. Conversely, the same REDOR experiments with use of distearoylphosphatidylcholine (DSPC) showed no dephasing for the C39/C40 methyl signals while a marked reduction of the C41 carbonyl signal was again observed. These findings should be most reasonably accounted for by the notion that AmB can span across the DMPC membrane with a single-length interaction but cannot span the DSPC membrane due to its greater thickness. To our knowledge, the results provide the first direct spectroscopic evidence for the formation of a single-length channel across a biomembrane, which was previously suggested by channel current recording experiments.

Amphotericin B (AmB),[1] a polyene antibiotic produced by *Streptomyces nodosus*, is clinically used for the treatment of systemic fungal infections (*1*, *2*). Its molecular structure (Figure 1a) was elucidated by X-ray crystallographic analysis for an *N*-iodoacetyl derivative to be a glycosylated 38-membered lactone encompassing an amphiphilic polyhydroxy part, a conjugated heptaene chromophore, and an amphoteric ion pair (*3*, *4*). It is generally accepted that an ion-permeable channel formed across the bilayer membrane is responsible for the biological activity of AmB (*5*, *6*). In the well-known "barrel-stave" hypothesis, about eight molecules of AmB form an ion channel, in which the polyhydroxy region of AmB composes the lining of a channel pore while its heptaene is radialized to interact with the hydrophobic membrane interior (*7*, *8*). Single channel recording experiments have revealed that ion-permeable channels formed by AmB can be categorized into five or more subtypes according to conductance (*9*−*11*). These multiple channels could be roughly grouped into two classes: one is a single-length channel, a single molecule to span the membrane, and the other is a double-length channel, two molecules to span the membrane (*12*, *13*) (see Figure 7). The length of AmB along the molecular long axis is reported to be ca. 24 Å (*3*, *4*). The thickness of typical biomembranes mainly consisting of phospholipids is around 35 Å, which comprises 8 Å of the hydrophilic headgroup and 27 Å of the hydrophobic region (*14*). Simple comparison of these lengths suggests that a double molecular length may be necessary for AmB to pierce through the whole membrane while a single molecular length can barely penetrate the hydrocarbon region of acyl chains. Recently, our results of channel activities for mixed PC membranes (*15*) showed that a single molecule of AmB could possibly span the hydrophobic thickness of bilayer membranes consisting of saturated $C_{10}-C_{14}$ fatty acyl groups. However, no direct evidence has hitherto been obtained as to whether a single-length or double-length channel of AmB predominantly occurs in the biomembrane.

Besides polyene antibiotics, a great variety of drugs and natural products are known to interact with membrane proteins and/or membrane lipids upon exerting their biological activities. Molecular recognition occurring in the membrane should provide invaluable information on the mechanism of action by membrane-bound drugs and functions of membrane-integral biomolecules. However, it is extremely difficult to elucidate the precise structure of membrane-embedded complexes mainly due to a lack of methodology; the two major methods in structural biology, X-ray crystal-

† This work was supported by a Grant-in-Aid for Scientific Research on Priority Area (A) (No. 12045243) from the Ministry of Education, Culture, Sports, Sciences, and Technology, Japan, by a grant from the CREST, Japan Science and Technology Corporation, and by the Yamada Science Foundation.

* To whom correspondence should be addressed. Phone/Fax: +81-66850-5774. E-mail: murata@ch.wani.osaka-u.ac.jp.

‡ Osaka University.

§ CREST.

[1] Abbreviations: AmB, amphotericin B; DMPC, 1,2-dimyristoyl-*sn*-glycero-3-phosphocholine; DSPC, 1,2-distearoyl-*sn*-glycero-3-phosphocholine; HEPES, 2-[4-(2-hydroxyethyl)-1-piperazinyl]ethanesulfonic acid; MAS, magic angle sample spinning; NMR, nuclear magnetic resonance; PC, phosphatidylcholine; POPC, 1-palmitoyl-2-oleoyl-*sn*-glycero-3-phosphocholine; REDOR, rotational echo double resonance.

10.1021/bi049001k CCC: $30.25 
Published on Web 12/18/2004

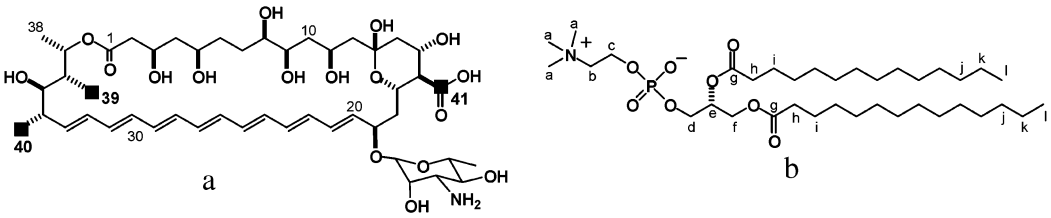

FIGURE 1: (a) Labeled carbons of [tri-$^{13}$C]AmB are indicated with solid squares. (b) $^{13}$C assignment of 1,2-dimyristoyl-*sn*-glycero-3-phosphocholine (DMPC) (*26*) (see Figures 2 and 3).

lography and solution NMR, are rather powerless for membrane-bound entities. Recently, technological advance in solid-state NMR spectroscopy greatly enhances its utility for the structural elucidation of biological molecules (*16*, *17*). For investigating interactions between phospholipids and membrane-bound molecules including integral peptides/proteins, paramagnetic multivalent cations such as $Mn^{2+}$, $Dy^{3+}$, and $Gd^{3+}$ have been often used to estimate the depth from the bilayer surface (*18*−*20*). Another technique in solid-state NMR is based on the magnetization of $^{31}$P in phospholipids as reported by Hirsh et al. (*21*). Since $^{2}$H NMR studies have revealed that AmB immobilizes phospholipid in a molar ratio of approximately 1:1 (*22*), their lateral diffusion may be restricted to some extent, which is expected to enhance the intermolecular dipolar interactions. Thus the $^{31}$P nucleus of the phospholipid should give rise to measurable intermolecular dipolar interaction with a labeled atom in AmB. For the selective detection of weak heteronuclear dipolar coupling in the lipid membrane samples, rotational echo double resonance (REDOR) is the method of choice (*21*, *23*).

We wish to report an application of solid-state NMR experiments for studying the molecular interaction between membrane-bound AmB and membrane lipids, which provides evidence that the drug spans across biomembrane-mimicking DMPC bilayers with a single-length interaction.

## MATERIALS AND METHODS

*Materials.* Phospholipids, 1,2-dimyristoyl-*sn*-glycero-3-phosphocholine (DMPC) and 1,2-distearoyl-*sn*-glycero-3-phosphocholine (DSPC), were purchased from Avanti Polar Lipid Inc. (Alabaster, AL) and Wako Pure Chemical Industries (Osaka, Japan), respectively. Authentic AmB and Aliquat 336 (Acros Organics) were purchased from Wako Pure Chemical Industries (Osaka, Japan). Propionic-3-$^{13}$*C* acid sodium salt (ICON), synonymous with [3-$^{13}$C]propionate, was obtained from Shodex (Tokyo, Japan). All of these chemicals were used without further purification.

*Culture of S. nodosus and Extraction of AmB. S. nodosus* obtained from American Type Culture Collection (ATCC 14899) was cultured as reported by McNamara et al. (*24*) to produce [tri-$^{13}$C]AmB. For the production culture, *S. nodosus* was grown on a medium containing fructose, 20 g/L, dextrin, 60 g/L, soy bean flower, 30 g/L, and $CaCO_3$, 10 g/L (pH 7.0) (*24*). A 500 mL Erlenmyer flask containing production medium (50 mL) was incubated at 26 °C with shaking at 200 rpm. Sodium [3-$^{13}$C]propionate (350 mg) was added to the medium seven times in equal aliquots of 50 mg in 200 $\mu$L of sterile water over 70 h. After 120 h incubation, the harvested broth was adjusted to pH 10.5 with 5 M NaOH (0.5 mL/50 mL of broth), and then 25 mL of ethyl acetate containing Aliquat 336 (7% w/v) was added. After being stirred vigorously for 1 h (200 rpm), the broth was again adjusted to pH 10.5 by 5 M NaOH. After centrifugation (8000*g*, 10 min), the organic phase was collected by decantation and cooled to 4 °C for 1 week to precipitate AmB as yellow solids. The precipitate was collected by centrifugation, washed with acetone (3 mL), dry acetone (3 mL), and methanol (3 mL), and then dried under vacuum to give amorphous AmB (*24*). For complete removal of Aliquat 336, AmB was dissolved in DMF (2 mL) containing acetic acid (25 $\mu$L, pH 4), and then diethyl ether (10 mL) was added to precipitate AmB. Purified AmB was collected by decantation and dried under vacuum to furnish an average of 20 mg of AmB from 50 mL of the culture. The purity was checked by $^{13}$C NMR (>95%). The average incorporation of $^{13}$C at C39, C40, and C41 was estimated to be 15%.

*Solid-State NMR Measurements.* For preparing membrane-bound AmB, 4 mg of [tri-$^{13}$C]AmB and 29 mg of DMPC (molar ratio 1:10) were mixed in $CHCl_3$/MeOH (6/1), and the solvent was removed in vacuo for 8 h. The membrane preparation was hydrated with 33 $\mu$L of 10 mM HEPES buffer (pH 7.0) under Ar and then diluted with 1 mL of $H_2O$. After sonication for a few minutes, the membrane was freeze−thawed and stirred vigorously to make multilamellar vesicles. The suspension was lyophilized, rehydrated with $D_2O$, and packed into a $\phi$ 4 mm MAS rotor. The sampling for [tri-$^{13}$C]AmB/DSPC (1/10) was carried out in the same way. $^{13}$C−$^{31}$P REDOR spectra (*23*) were recorded at 75.315 MHz for $^{13}$C on a CMX300 (Varian/Chemagnetics) spectrometer with the MAS frequency of 7000 ± 2 Hz. The rotor temperature was maintained at 30 ± 1 °C by a temperature controller. The spectral width was 30 kHz. Typically, the $\pi/2$ pulse width for $^{1}$H was 3 $\mu$s, and $\pi$ pulse widths for $^{13}$C and $^{31}$P were 6 and 9 $\mu$s, respectively. The contact time for cross-polarization transfer was set to be 2 ms. Spectra were acquired with a recycle delay of 5 s and a $^{1}$H decoupling field strength of 83 kHz. REDOR spectra were measured at two dephasing times, 11.4 and 22.9 ms, using xy-8 phase cycling for $^{31}$P irradiations (*25*). Static $^{31}$P NMR spectra were recorded without MAS to confirm the phase status of PC in a sample.

## RESULTS

*REDOR Dephasing Effects Observed for Carbon Atoms of the Membrane Lipid.* Figure 2 shows a set of $^{13}$C−$^{31}$P REDOR spectra of the [tri-$^{13}$C]AmB/DMPC with 160 rotor cycles (dephasing time 22.9 ms). The full-echo spectrum shows narrow peaks for natural abundance $^{13}$C atoms of DMPC (signals a−l), where signal assignments are based on reference data (*26*). Typical line half-widths of the DMPC signals are 20−36 Hz. In the difference spectrum large peaks for a methylene of choline (c) and glycerol (d−f) are observed. The lack of REDOR dephasing at the terminal part

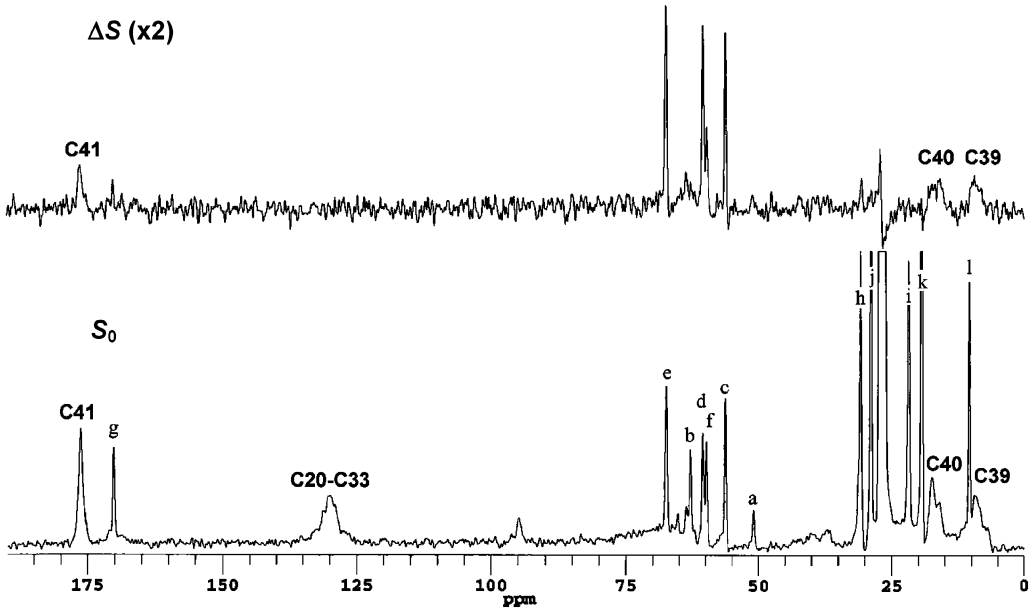


FIGURE 2: $^{13}C-^{31}P$ REDOR spectra of [tri-$^{13}C$]AmB in DMPC. The membrane preparation contained the $^{13}C$-labeled AmB at an AmB/DMPC molar ratio of 1/10 and 50 wt % 10 mM HEPES/$D_2O$ buffer (pH 7.0). The spectra were obtained after 160 rotor cycles of $^{31}P$ dephasing (22.9 ms) with the magic angle spinning at 7 kHz at 30 °C. The number of the scans accumulated for the full echo spectrum, $S_0$, was 61440. The top trace is a REDOR difference spectrum, $\Delta S$. All signals from both ends of [tri-$^{13}C$]AmB, C39, C40, and C41, show significant dipolar coupling upon irradiating the $^{31}P$ resonance of DMPC. On the other hand, the signals from the heptaene C20−33 residing in the middle of the molecule are not reduced.

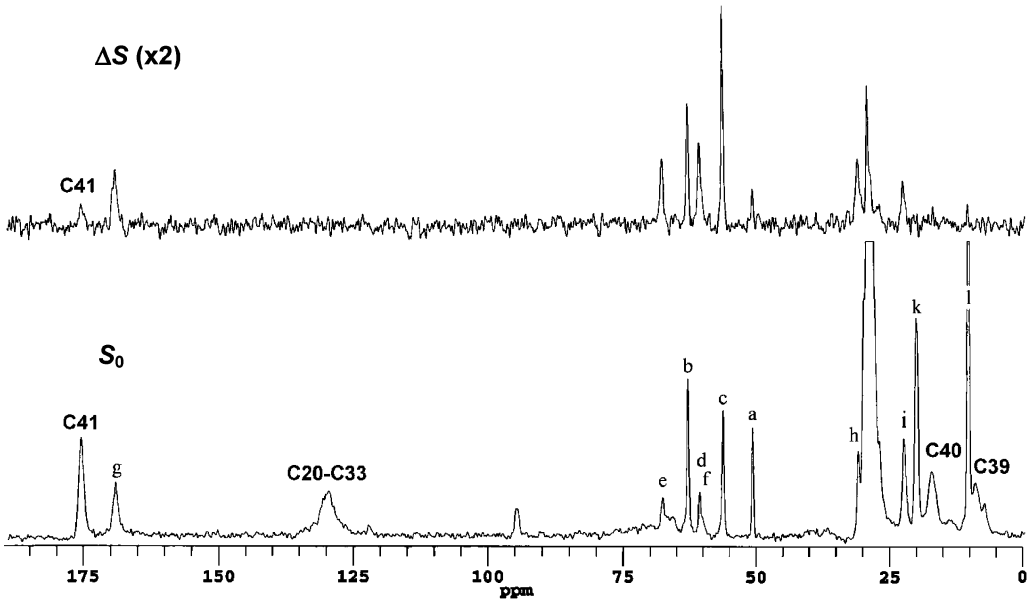


FIGURE 3: $^{13}C-^{31}P$ REDOR spectra of [tri-$^{13}C$]AmB in DSPC. The membrane preparation contained the $^{13}C$-labeled AmB at an AmB/DMPC molar ratio of 1/10 and 50 wt % 10 mM HEPES/$D_2O$ buffer (pH 7.0). The spectra were obtained after 160 rotor cycles of $^{31}P$ dephasing (22.9 ms) with the magic angle spinning at 7 kHz at 30 °C. The number of the scans accumulated for the full echo spectrum, $S_0$, was 30976. The top trace is the REDOR difference spectrum, $\Delta S$. The signal of C41 residing at the tail end of [tri-$^{13}C$]AmB shows significant dipolar dephasing with $^{31}P$ of DSPC while the signals of C20−33, C39, and C40 from the hydrophobic parts of the molecule stay unchanged.

of acyl chain (k, l) is in agreement with the bilayer structure (*27*). The magnitude of the chemical shift anisotropy of static $^{31}P$ NMR was 43 ppm with the line width at half-height of 1.5 kHz, which coincides with the value for the pure DMPC bilayer membrane in the liquid-crystalline ($L_\alpha$) phase (*28*).

Figure 3 shows the $^{13}C-^{31}P$ REDOR spectra of DSPC in the presence of AmB recorded for 160 rotor cycles. Carbon atoms at natural abundance give rise to broader peaks (27−90 Hz) than those of DMPC. The REDOR difference spectrum of the DSPC membrane shows large dephasing for choline (a−c), glycerol (d−f), and a part of the acyl chain close to the polar head (g−i). The lack of REDOR difference signals for the terminal part of the acyl chain (k, l) indicates that DSPC forms the bilayer (*27*). The static $^{31}P$ NMR of the AmB/DSPC has the chemical shift anisotropy of 58 ppm with the line width at half-height of 4.9 kHz, which is characteristic of that of the DSPC membrane in the gel ($L_{\beta'}$) phase (*28*). As depicted in Figure 4, the REDOR dephasing effects are more prominent for the DSPC than DMPC membrane, which is in good agreement with the results of

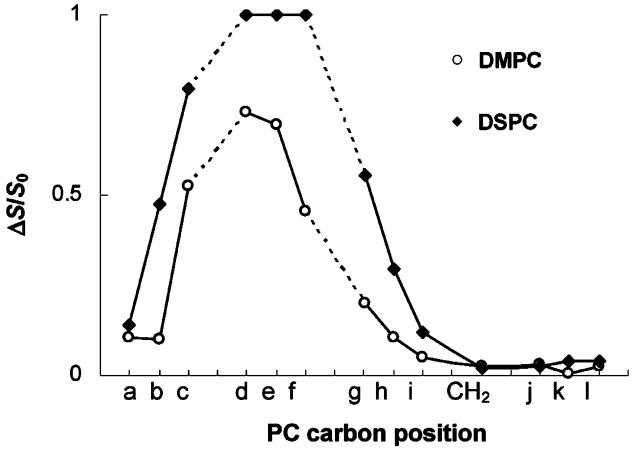


FIGURE 4: $^{13}C-^{31}P$ REDOR dephasing observed on natural abundance carbon atoms of DMPC and DSPC. The *x*-axis represents the carbon positions of PC shown in Figure 1. The *y*-axis is a REDOR dephasing shown as the ratio $\Delta S/S_0$ in $^{13}C$ NMR peak areas between the full echo and REDOR difference spectra after 160 rotor cycles of $^{31}P$ dephasing (22.9 ms), which are shown in Figures 2 and 3.

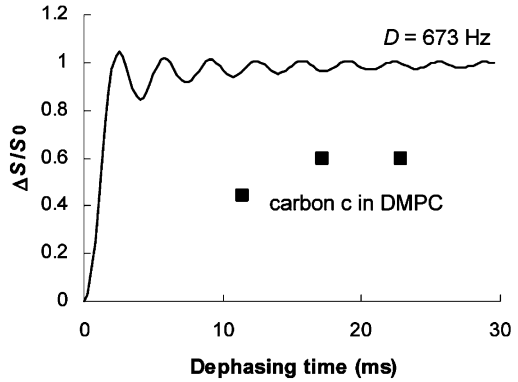


FIGURE 5: $^{13}C-^{31}P$ REDOR dephasing ($\Delta S/S_0$) of the natural abundance carbon c of DMPC, which has a fixed $^{13}C-^{31}P$ distance (2.63 Å) in the DMPC molecule (*35*). Solid squares show apparent REDOR depahsing from experiments. The line shows the ideal REDOR dephasing curve for the $^{13}C-^{31}P$ spin pair in static sample with the internuclear distance of 2.63 Å, which corresponds to the dipolar coupling constant of 673 Hz. The REDOR dephasing in fluid lipid is significantly attenuated by its high molecular mobility.

$^{31}P$ NMR; the increased dynamics of the liquid-crystalline phase attenuate the dipolar coupling more effectively than that of the gel phase and thus yield less REDOR dephasing for the same distances.

Figure 5 shows the REDOR dephasing for one of the shortest $^{13}C-^{31}P$ distances in the DMPC molecule (carbon c, $r_{CP}$ = 2.63 Å). The result shows significantly less dephasing than the expected REDOR curve for a $^{13}C-^{31}P$ spin pair in the solid-state sample with the same distance. This attenuation is caused by some molecular motions of DMPC, e.g., the axial rotation and its tilt motion, intramolecular motions due to conformational changes, and the lateral diffusion on vesicles in various sizes.

*$^{13}C-^{31}P$ Dipolar Interaction between AmB and DMPC in the Membrane.* Figure 1 illustrates the labeled positions of [tri-$^{13}C$]AmB obtained from the culture of *S. nodosus*. Three isolated $^{13}C$ nuclei at the both ends of AmB were labeled with [3-$^{13}C$]propionate as reported previously (*24*). [tri-$^{13}C$]-AmB incorporated into the DMPC membrane ($C_{14}$ acyl chains) was subjected to $^{13}C-^{31}P$ REDOR experiments.

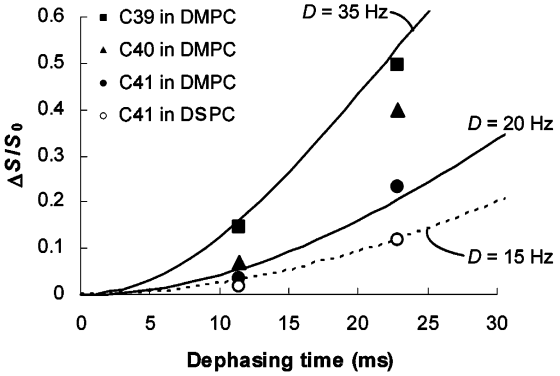


FIGURE 6: $^{13}C-^{31}P$ REDOR dephasing ($\Delta S/S_0$) of the labeled carbons on [tri-$^{13}C$]AmB as a function of the dipolar evolution time in DMPC (solid symbols) and in DSPC (open circles). The lines show the ideal REDOR dephasing curves for static two-spin systems.

Figure 2 shows $^{13}C-^{31}P$ REDOR spectra of [tri-$^{13}C$]AmB/DMPC after 160 rotor cycles. The labeled AmB gave rise to four broad signals in the full-echo spectrum (C20−C33, C39, C40, C41). Although the olefinic carbons in C20−C33 are not labeled with [3-$^{13}C$]propionate, 14 carbon atoms at natural $^{13}C$ abundance pile up to form a broad peak. In the difference spectrum (Figure 2), three peaks for the labeled positions, C39, C40, and C41, are clearly shown with $\Delta S/S_0$ of 0.50, 0.40, and 0.23, respectively, demonstrating the close interaction between AmB and DMPC where both ends of AmB come close to the phosphate ester of DMPC. These observations support the formation of single-length channels but not double-length ones in the DMPC bilayer (Figure 7) (*12*, *13*). On the other hand, the C20−C33 carbons residing in the middle part of the molecule give rise to no detectable peaks in the difference spectrum. The data rule out the possibility that AmB lies on the DMPC bilayer keeping the heptaene part in a parallel position to the membrane surface. Both C39 and C40 show at least two isotropic chemical shifts, which implies that AmB takes two or more forms in the DMPC bilayer. These multiple forms may well be distinguishable by NMR spectra because the lifetime of at least four types of ion channels is reported to be longer than some 10 ms by single channel recording experiments (*10*).

*$^{13}C-^{31}P$ Dipolar Interaction between AmB and DSPC in the Membrane.* In the next experiments, the $^{13}C-^{31}P$ interactions were examined for thicker membrane consisting of DSPC with $C_{18}$ acyl chains. $^{13}C-^{31}P$ REDOR spectra after 160 rotor cycles are shown in Figure 3. In the full-echo spectrum, four broad signals are observed for [tri-$^{13}C$]AmB (C20−C33, C39, C40, and C41). Two or more isotropic chemical shifts for C39 again indicate that AmB has multiple forms in the DSPC membrane (*10*). The REDOR dephasing effects are, however, markedly different from those in DMPC. [tri-$^{13}C$]AmB in the DSPC membrane gives rise to only a difference signal for C41 at the polar end (Figure 3) while all of the three labeled carbons at both ends of AmB (C39, C40, C41) appear in the spectrum of DMPC (Figure 2). REDOR difference is not observable for the heptaene region (C20−C33) as is the case with the DMPC membrane. These findings may support the model that AmB interacts with the headgroup of DSPC with a polar terminal part and penetrates into the interior of DSPC bilayers without reaching the opposite side of the membrane (Figure 7).

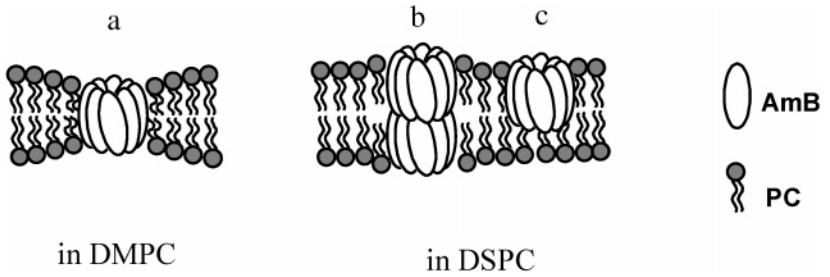


FIGURE 7: Schematic models for AmB−DMPC and AmB−DSPC interactions in the bilayer membrane. The results of $^{13}C-^{31}P$ REDOR experiments in the DMPC bilayer agree with the single-length complex (a), one molecule to span the membrane. The double-length complex (b) and/or the single-length complex (c) not reaching the other side are probably dominant in the DSPC bilayer.

## DISCUSSION

The present results of $^{13}C-^{31}P$ REDOR experiments have disclosed that AmB interacts with membrane lipids in two ways, the single length or the double length, either of which possibly occurs in membrane depending on the thickness of bilayers (Figure 7). Channel current recording studies have suggested that AmB can form both types of a single-length and double-length channels in the biological membrane with different channel conductance (*9*−*11*). The coexistence of the two channels can plausibly account for the complicated AmB activity in membrane permeabilization although no direct spectroscopic evidence has so far been obtained. The present study succeeded in observing the direct interactions between the tail end of AmB and the headgroup of PC; to our knowledge, these interactions may be the first unambiguous spectroscopic evidence supporting a single-length channel formed by AmB.

The length of a hydrophobic part of AmB encompassing the conjugated heptaene group is 22 Å (*13*) while the lengths of hydrocarbon chains in DMPC and DSPC bilayer at room temperature are 26 and 39 Å, respectively (*14*, *29*). A simple comparison of their hydrophobic lengths implies that a single-length channel can be formed in DMPC bilayers and a double-length channel in DSPC bilayers. This seems to be the case with the present results. It is noteworthy that ion channel formation by AmB is more significantly affected by the hydrophobic length than by the whole length; the former is usually smaller than the latter by around 10 Å (*15*). Most of the biomembranes take the liquid-crystal phase, and the thickness of the hydrophobic interior is roughly estimated to be 27 Å (*14*), which is comparable with that of DMPC. Thus, under physiological conditions, AmB should chiefly form a single-length channel, through which relatively large ion current elicits the pharmacological action of the drug (*9*, *10*).

For the DMPC membrane, the signal shapes of C39 and C40 in Figure 2 imply the presence of multiple isotropic chemical shifts, which should be due to multiple modes of molecular interactions involved in the AmB complex. Most of these interactions are thought to occur in the single-length complex because the $^{13}C-^{31}P$ REDOR dephasing effects are observed for all of the components of C39 and C40 signals. Similar observations have been reported by Cotero et al. that AmB forms two types of single-length channels with a different pore size (10).

In the present study, we successfully disclosed the membrane topology of bound AmB in the phospholipid bilayers using $^{13}C-^{31}P$ REDOR. In addition, more detailed discussion may be possible on the basis of the solid-state NMR data. If a two-spin system is assumed, which should be reasonable under the experimental conditions, apparent dipolar coupling constants between the $^{13}C$-labeled position and phosphate in PCs are estimated to be 15−35 Hz (Figure 6). Apparent dipolar coupling constants observed in the phospholipid membrane should be attenuated from those in the solid state because of various molecular motions as depicted in Figure 5; axial rotation, tilting motion, conformational change, and lateral diffusion on bilayer vesicles considerably contribute to the time averaging and/or distribution of dipolar interaction. In the case of intermolecular dipolar coupling between AmB and PC, the fluctuation of $^{13}C-^{31}P$ distance, in addition to these motions, further reduces the values. The data acquired in this study may not be enough to accurately determine the $^{13}C-^{31}P$ distances in such a complicated system. It may be, however, possible to discuss AmB−PC interaction by using the minimum values of the dipolar coupling constants obtained from the REDOR data. According to Figure 6, the minimum values for C39, C40, and C41 in the DMPC membrane, which should be obtained under the assumption that neither AmB nor PC undergoes molecular motions, are about 35, 30, and 20 Hz, respectively. These dipolar coupling constants correspond to the maximum $^{13}C-^{31}P$ distances of 7.1, 7.4, and 8.4 Å, respectively. The cross-section areas of AmB and DMPC are reported to be 36 and 60 $Å^2$, and their average radii should be 3.4 and 4.4 Å (*14*, *32*). If AmB and DMPC undergo each fast axial rotation around the bilayer normal (*31*), the average distance between the AmB and PC molecular center would be about 7.8 Å. The notion indicates that, even with the maximum distance, AmB and DMPC reside very closely, probably in direct contact.

Along the vertical axis, the ammonium group of AmB and the phosphate of PC are thought to be in the vicinity as reported previously (*33*, *34*). Moreover, when considering the closeness between C39/C40/C41 of AmB and the phosphate of PC on the lateral axis as discussed above, their distance in the vertical direction or in other words "difference in depth" should also be small, hence demonstrating that both termini of AmB come close to the surface of the PC membrane. Under the experimental conditions, the attenuation of dipolar coupling by other molecular motions should also be taken into consideration; in particular, if the exchange of the DMPC molecule paired with AmB takes place due to the fast lateral diffusion (*30*), intermolecular dipolar couplings should be much reduced. Thus the present results indicate that, in addition to the single channel orientation of

AmB in DMPC, the AmB−DMPC complex is very stable, whose lifetime may be longer than the time scale of dipolar coupling.

In terms of efficiency in $^{13}C-^{1}H$ cross-polarization, we initially thought that AmB in the DSPC membrane should show larger $^{13}C-^{31}P$ dipolar coupling than in DMPC membrane because of the restricted molecular motion in the gel-phased DSPC membrane as implied in Figure 4. The observed $^{13}C-^{31}P$ REDOR dephasing between AmB and PC, however, was smaller in the DSPC membrane. As mentioned above, there are some possible accounts. Unlike the DMPC membrane, the hydrophobic length of the DSPC bilayer does not fit that of the AmB molecule, which affects the fluctuation of $^{13}C-^{31}P$ distance and its angle to the rotation axis. Another possibility is that AmB in DSPC has interaction with PC at one side while AmB in DMPC interacts at both sides of the membrane, which elicits a faster tumbling of an AmB molecule in the DSPC membrane.

$^{13}C$-Labeled AmB at both sides of the molecule is a versatile tool for studying the membrane topology of the drug using $^{13}C-^{31}P$ REDOR, while providing limited information about the structure of the membrane complex. REDOR experiments using uniformly labeled AmB are currently underway.

## ACKNOWLEDGMENT

We are grateful to Prof. Yuzuru Mikami, Research Center for Pathogenic Fungi and Microbial Toxicoses, Chiba University, for antifungal assays, to Prof. Tohru Oishi for discussion, and to Mutsuhiro Ohata and Yuichi Umegawa for help in cultures of the microorganism.

## REFERENCES

1. Gallis, H. A., Drew, R. H., and Pickard, W. W. (1990) Amphotericin B: 30 years of clinical experience, *Rev. Infect. Dis. 12*, 308−329.
2. Hann, I. M., and Prentice, H. G. (2001) Lipid-based amphotericin B: a review of the last 10 years of use, *Int. J. Antimicrob. Agents 17*, 161−169.
3. Mechlinski, W., Schaffner, C. P., Ganis, P., and Avitabile, G. (1970) Structure and absolute configuration of the polyene macrolide antibiotic amphotericin B, *Tetrahedron Lett. 44*, 3873−3876.
4. Ganis, P., Avitabile, G., Mechlinski, W., and Schaffner, C. P. (1971) Polyene macrolide antibiotic amphotericin B. Crystal structure of the N-iodoacetyl derivative, *J. Am. Chem. Soc. 93*, 4560−4564.
5. Bolard, J. (1986) How do the polyene macrolide antibiotics affect the cellular membrane properties?, *Biochim. Biophys. Acta 864*, 257−304.
6. Hartsel, S., and Bolard, J. (1996) Amphotericin B: new life for an old drug, *Trends Pharmacol. Sci. 17*, 445−449.
7. De Kruijff, B., and Demel, R. A. (1974) Polyene antibiotic-sterol interactions in membranes of *Acholeplasma laidlawii* cells and lecithin liposomes. 3. Molecular structure of the polyene antibiotic-cholesterol complexes, *Biochim. Biophys. Acta 339*, 57−70.
8. Baginski, M., Resat, H., and Borowski, E. (2002) Comparative molecular dynamics simulations of amphotericin B-cholesterol/ergosterol membrane channels, *Biochim. Biophys. Acta 1567*, 63−78.
9. Brutyan, R. A., and McPhie, P. (1996) On the one-sided action of amphotericin B on lipid bilayer membranes, *J. Gen. Physiol. 107*, 69−78.
10. Cotero, B. V., Rebolledo-Antunez, S., and Ortega-Blake, I. (1998) On the role of sterol in the formation of the amphotericin B channel, *Biochim. Biophys. Acta 1375*, 43−51.
11. Venegas, B., Gonzalez-Damian, J., Celis, H., and Ortega-Blake, I. (2003) Amphotericin B channels in the bacterial membrane: Role of sterol and temperature, *Biophys. J. 85*, 2323−2332.
12. Marty, A., and Finkelstein, A. (1975) Pores formed in lipid bilayer membranes by nystatin. Differences in its one-sided and two-sided action, *J. Gen. Physiol. 65*, 515−526.
13. Kleinberg, M. E., and Finkelstein, A. (1984) Single-length and double-length channels formed by nystatin in lipid bilayer membranes, *J. Membr. Biol. 80*, 257−269.
14. Petrache, H. I., Tristram-Nagle, S., and Nagle, J. F. (1998) Fluid phase structure of EPC and DMPC bilayers, *Chem. Phys. Lipids 95*, 83−94.
15. Matsuoka, S., and Murata, M. (2003) Membrane permeabilizing activity of amphotericin B is affected by chain length of phosphatidylcholine added as minor constituent, *Biochim. Biophys. Acta 1617*, 109−115.
16. Luca, S., Heise, H., and Baldus, M. (2003) High-resolution solid-state NMR applied to polypeptides and membrane proteins, *Acc. Chem. Res. 36*, 858−865.
17. Thompson, L. K. (2002) Solid-state NMR studies of the structure and mechanisms of proteins, *Curr. Opin. Struct. Biol. 12*, 661−669.
18. Villalain, J. (1996) Location of cholesterol in model membranes by magic-angle-sample-spinning NMR, *Eur. J. Biochem. 241*, 586−593.
19. Grobner, G., Glaubitz, C., and Watts, A. (1999) Probing membrane surfaces and the location of membrane-embedded peptides by $^{13}C$ MAS NMR using lanthanide ions, *J. Magn. Reson. 141*, 335−339.
20. Tuzi, S., Hasegawa, J., Kawaminami, R., Naito, A., and Saito, H. (2001) Regio-selective detection of dynamic structure of transmembrane alpha-helices as revealed from $^{13}C$ NMR spectra of [3-$^{13}C$]Ala-labeled bacteriorhodopsin in the presence of $Mn^{2+}$ ion, *Biophys. J. 81*, 425−434.
21. Hirsh, D. J., Hammer, J., Maloy, W. L., Blazyk, J., and Schaefer, J. (1996) Secondary structure and location of a magainin analogue in synthetic phospholipid bilayers, *Biochemistry 35*, 12733−12741.
22. Dufourc, E. J., Smith, I. C., and Jarrell, H. C. (1984) Interaction of amphotericin B with membrane lipids as viewed by $^{2}H$-NMR, *Biochim. Biophys. Acta 778*, 435−442.
23. Gullion, T., and Schaefer, J. (1989) Rotational-echo double-resonance NMR, *J. Magn. Reson. 81*, 196−200.
24. McNamara, C. M., Box, S., Crawforth, J. M., Hickman, B. S., Norwood, T. J., and Rawlings, B. J. (1998) Biosynthesis of amphotericin B, *J. Chem. Soc., Perkin Trans. 1*, 83−87.
25. Gullion, T., Baker, D. B., and Conradi, M. S. (1990) New, compensated Carr-Purcell sequences, *J. Magn. Reson. 89*, 479−484.
26. Lee, C. W. B., and Griffin, R. G. (1989) Two-dimensional $^{1}H/^{13}C$ heteronuclear chemical shift correlation spectroscopy of lipid bilayers, *Biophys. J. 55*, 355−358.
27. Hirsh, D. J., Lazaro, N., Wright, L. R., Boggs, J. M., McIntosh, T. J., Schaefer, J., and Blazyk, J. (1998) A new monofluorinated phosphatidylcholine forms interdigitated bilayers, *Biophys. J. 75*, 1858−1868.
28. Cullis, P. R., De Kruyff, B., and Richards, R. E. (1976) Factors affecting the motion of the polar headgroup in phospholipid bilayers. A phosphorus-31 NMR study of unsonicated phosphatidylcholine liposomes, *Biochim. Biophys. Acta 426*, 433−446.
29. Sun, W.-J., Tristram-Nagle, S., Suter, R. M., and Nagle, J. F. (1996) Structure of gel phase saturated lecithin bilayers: Temperature and chain length dependence, *Biophys. J. 71*, 885−891.
30. Watts, A. (1998) Solid-state NMR approaches for studying the interaction of peptides and proteins with membranes, *Biochim. Biophys. Acta 1376*, 297−318.
31. Hing, A. W., Schaefer, J., and Kobayashi, G. S. (2000) Deuterium NMR investigation of an amphotericin B derivative in mechanically aligned lipid bilayers, *Biochim. Biophys. Acta 1463*, 323−332.
32. Gruszecki, W. I., Gagos, M., and Kernen, P. (2002) Polyene antibiotic amphotericin B in monomolecular layers: spectropho-

tometric and scanning force microscopic analysis, *FEBS Lett. 524*, 92−96.
33. Balakrishnan A. R., and Easwaran K. R. K. (1993) Lipid-amphotericin B complex structure in solution: A possible first step in the aggregation process in cell membranes, *Biochemistry 32*, 4139−4144.
34. Matsuoka, S., Matsumori, N., and Murata, M. (2003) Amphotericin B phospholipid covalent conjugates: dependence of membrane-permeabilizing activitiy on acyl-chain length, *Org. Biomol. Chem. 1*, 3882−3884.
35. Pascher, I., and Sundell, S. (1986) Membrane lipids: preferred conformational states and their interplay. The crystal structure of dilauroylphosphatidyl-N,N-dimethylethanolamine, *Biochim. Biophys. Acta 855*, 68−78.

BI049001K